Characteristics and synergistic effects of co-pyrolysis of microalgae with polypropylene

Liyang Jiang[a], Zhen Zhou[a], Huan Xiang[b], Yang Yang[b], Hong Tian[a,*], Jiawei Wang[b,*]

a School of Energy & Power Engineering, Changsha University of Science & Technology, Changsha, 410114, China

b Bioenergy Research Group, EBRI, Aston University, Birmingham, B4 7ET, UK

corresponding author: Hong Tian (tianh1103@163.com), Jiawei Wang (j.wang23@aston.ac.uk)

Abstract

To further improve the quality of microalgae-derived bio-oil, the characteristics, kinetic parameters and product distribution of the co-pyrolysis of polypropylene (PP) and Chlorella vulgaris (C.V) were studied by thermogravimetric analysis (TGA) and pyrolysis gas chromatography/mass spectrometry (Py-GC/MS). The TGA results showed that with the increase of the PP amount, the peak temperature of maximum pyrolysis weight loss of C.V decreased, but the trend of PP was opposite. Compared with the experimental and theoretical values, it was found that the residual amount of solid coke and the total activation energy required for co-pyrolysis were significantly reduced, which indicated that there was an obvious synergistic effect during the co-pyrolysis process. The Py-GC/MS results showed that when the PP mass ratio was 0.75 and the final pyrolysis temperature was 500 ℃, the reaction activation energy and

hydrocarbon yield had the best synergistic effect. Moreover, the co-pyrolysis of C.V and PP promoted the formation of aliphatic hydrocarbons, inhibited the aromatisation and Maillard reactions, and hindered the formation of aromatics, nitrogenous compounds, acids and oxides.

Keywords: Chlorella vulgaris; polypropylene; co-pyrolysis; kinetic parameter; Py-GC/MS ; synergistic effect

1 Introduction

With the continuous growth of population and the expansion of modern industrialisation, the problems of global energy shortage and environmental pollution are becoming increasingly serious. It is urgent to find renewable and clean energy [1,2]. At present, biomass is considered as an energy substitute with a virtuous cycle of environmental protection and economic development requirements. As the third generation biomass, microalgae is the most promising alternative energy in biomass resources due to many advantages, such as short growth cycle, high photosynthetic efficiency, strong CO_2 storage capacity, high oil production rate, and friendly living environment [3,4]. Pyrolysis of microalgae to produce bio-oil is a technology with great application prospects. The bio-oil typically has a high yield (41.1-64.9%) and higher heating value (HHV:27.15-32.1MJ/kg), while only a small amount of useless and harmful residues are found (15-28wt%)[5]. Meanwhile, Teng et al. [6] investigated the pyrolysis of *Chlorella vulgaris*. The results showed that the maximum pyrolysis mass loss of *Chlorella vulgaris* occurred at 190-600℃, and the solid residue decreased with the increase of pyrolysis heating rate. However, the production of hydrocarbons in the bio-oil is hindered due to the lack of hydrogen during the pyrolysis of microalgae, resulting in high oxygen and nitrogen contents in the bio-oil. As a result, the obtained bio-oil is strongly corrosive and shows high viscosity and poor fluidity and stability [7, 8].

In order to improve the quality and yield of microalgae pyrolysis products, many research work has been carried out. For example, catalytic cracking and

hydrodeoxygenation can improve the quality of bio-oil by promoting microalgae deoxygenation and denitrification. However, since hydrogen is used in the hydrodeoxygenation process, its safety requirements and operating costs are high, while catalytic pyrolysis has some shortcomings like expensive catalyst raw materials, complex catalyst preparation and operation procedures, and easy deactivation of the catalyst [9-11]. In recent years, co-pyrolysis has been widely used to improve the quality of pyrolysis fuel due to its advantages of simple operation, high efficiency and strong synergistic effect. Chen & Bong et al. [12,13] studied the co-pyrolysis of bamboo chips, peanut shell and microalgae. It was shown that the co-pyrolysis of microalgae and peanut shell can significantly reduce the reaction activation energy of individual pyrolysis. The ratio of bamboo chips and microalgae was 1:3, they had the best synergistic effect. Chen et al. [14] investigated the co-pyrolysis of *Chlorella* and kitchen waste by TG-FTIR and Py-GC/MS. The results indicated that the main pyrolysis temperature range of microalgae moved to lower values, and the apparent pyrolysis activation energy decreased while the content of hydrocarbons increased. Duan et al. [15] studied the co-pyrolysis of microalgae and waste tires. It was shown that co-pyrolysis promoted the deoxidation, desulfurisation and denitrification of products and reduced the pyridine derivatives and fatty acids in the bio-oil, and the obtained bio-oil had a high calorific value (35.80~42.03 MJ/kg). Xie et al.[16] investigated the effect of pyrolysis temperature and feedstock blending ratio on microwave co-pyrolysis of scum and microalgae. The study showed that the optimal blending ratio and pyrolysis temperature for bio-oil and aromatics production were 2:1

and 550℃, respectively. The synergistic effect of co-pyrolysis of scum and microalgae became more obvious when the effective hydrogen index (EHI) of feedstock was higher than 0.7.

According to statistics, China produced 63 million tons of waste plastics in 2019, and it is expected that the waste plastics in the ocean will exceed the number of fish by 2050 [17, 18]. At present, the treatment methods of plastics include landfill, incineration, composting, mechanical and chemical recycling. However, the landfill will cause soil pollution. Incineration will cause atmospheric pollution while composting will easily cause deterioration of groundwater quality. The crushing, melting and extrusion processes of mechanical recovery will lead to significant loss of chemical and physical properties compared to raw plastics[19]. At the same time, chemical recycling, such as pyrolysis, can convert plastics to high-value energy products [20]. Chen et al.[21] studied the co-pyrolysis of tobacco stems and polypropylene (PP). The results showed that the yield of organic gases increased, and the activation energy and residual biochar decreased. Besides, the calorific value of coke obtained by co-pyrolysis of pinecone and plastic was higher than that obtained by pyrolysis alone[22]. Burra et al. [23] investigated the kinetics of co-pyrolysis of pine and PP by TGA-DSC. They found that the co-pyrolysis of the two was mainly attributed to the fact that when PP melted, abundant hydrogen was provided for the decomposition of biomass, which improved the net carbon conversion efficiency and reduced the net carbon residue. In addition, Alam & Gu & Liew et al.[24-26] studied the co-pyrolysis of biomass (such as bamboo chips, waste wood chips, cotton stalks

97 and corn cobs) with hydrogen-rich waste plastics. The results showed that the
98 introduction of hydrogen-rich waste plastics into biomass decomposition could
99 improve the yield of aromatics and inhibit the formation of coke. Moreover, the
100 decarbonylation and decarboxylation reactions were replaced by the dehydration
101 reaction, which increased the H/C ratio of fuel and changed the reaction mechanism of
102 deoxygenation and thus improved the calorific value of the biofuel obtained. Kai &
103 Yuan & Majid et al. [27-29] found that HDPE promoted the pyrolysis of corn stalk and
104 *Chlorella vulgaris* during their co-pyrolysis process and also provided hydrogen for
105 biomass pyrolysis, which reduced the E_A and$\triangle H$, inhibited the formation of aldehydes,
106 ketones, furan groups and aliphatic hydrocarbons, and promoted the production of gas
107 volatiles and aromatic hydrocarbons. Dai & Cao et al. [30, 31] investigated the co-
108 pyrolysis of PVC and microalgae. The results showed that the contents of nitrogen-
109 containing and oxygen-containing organic compounds in liquid products decreased
110 significantly, while the contents of aromatics and calorific value of coke increased
111 significantly. Tang & Tang et al. [32, 33] reported that the co-pyrolysis of LDPE and
112 microalgae increased the gas yield and low calorific value, while the formation of N-
113 and O-containing compounds in the liquid was effectively inhibited. It also promoted
114 the dehydroxylation, ring-opening and hydrodeoxygenation reactions of the products,
115 which increased the yield of hydrocarbons. Therefore, it was demonstrated that the co-
116 pyrolysis of algae and plastic had the potential to improve the quality of bio-oil.

117 The nature of high H/C and low O/C ratios of plastics can make up for the lack of
118 hydrogen and enrichment of oxygen in microalgae, balance the content of C, H and O

elements in pyrolysis feedstock. Also, it can effectively reduce the production of wax compared to the pyrolysis of plastics alone, which can easily cause equipment blockage and shorten equipment life. Among all waste plastics, PP accounts for the highest proportion and contains nearly 14 wt. % of hydrogen, which can be considered as the best hydrogen source for biomass co-pyrolysis [34]. So far, only few reports on the co-pyrolysis characteristics and interaction mechanism of microalgae and PP plastics have been published, so it is necessary to carry out a further study. Therefore, in this work, PP and C.V were used as raw materials, and the effects of different mixing ratios of PP on the pyrolysis characteristics and product evolution of C.V were studied by TG and Py-GC/MS. At the same time, the theoretical and experimental values of pyrolysis kinetic parameters were compared to reveal the interaction of co-pyrolysis.

2 Experimental materials and methods

2.1 Materials

Chlorella Vulgaris (C.V) was purchased from Yunnan Baoshan Zeyuan Algae Industry Technology Co., Ltd. (China), and PP was purchased from Ningbo Zhizhan New Material Co., Ltd.(China). C.V and PP were ground and sieved to constant particle size (less than 120 μm). In order to obtain a uniform mixture, the two raw materials with PP-to-C.V ratios of 1:0, 3:1, 1:1, 1:3 and 0:1 were put into the agate mortar and stirred for 20 min until the colour of the samples was uniform. The proximate analysis and ultimate analysis of C.V and PP were carried out using a muffle furnace and Vario Marco Cube elemental analyser, respectively, and the results are presented in Table 1.

Table 1 Proximate and ultimate analysis of C.V and PP samples.

Sample	Ultimate Analysis[a] (wt.%)					Proximate Analysis[b] (wt.%)				HHV [c]
	C	H	O*	N	S	Volatile	Ash	Moisture	Fixed carbon	(MJ/kg)
C.V	48.30	7.15	35.04	9.01	0.50	65.85	8.82	7.71	17.62	21.58
PP	85.85	13.78	0.37	0.00	0.00	99.88	0.12	0.00	0.00	46.17

[a] Air dried basis. [b] Dry-ash free basis. [C] Higher heating value on dry basis. [*] Calculated by difference.

2.2 Co-pyrolysis experiments (TGA)

The co-pyrolysis experiments of PP and C.V were carried out using a thermogravimetric analyser (STA 499 TGA). Approximately 10 mg of sample was tested in each run. The sample was heated at a heating rate of 20 ℃/min, from room temperature to 900 ℃. Nitrogen with a purity of 99.999% and a flow rate of 50 mL/min was used to maintain an inert atmosphere.

2.3 Pyrolysis product analysis (Py-GC/MS)

The pyrolysis products of C.V and PP were analyze by Py-GC/MS. The Py-GC/MS was composed of the pyrolysis instrument of American CDS company and the gas-mass spectrometer of Shimadzu Company of Japan. The pyrolyzer was set at the heating rate of 10 ℃/ms, and maintained at the final temperature for 20 s. Firstly, the pyrolysis experiments of C.V were conducted at different final temperatures (300, 400, 500, 600 and 700 ℃), and found that the best pyrolysis temperature was 500 ℃. The mixtures of C.V and PP with different ratios (C.V:PP = 1:0, 3:1, 1:1, 1:3 and 0:1) were used as feedstocks for co-pyrolysis at 500 ℃ with an injection volume of 2 mg. The GC column was Rtx-5 (30 m × 0.25 mm × 0.25 μm). The column oven temperature was maintained at 40 ℃ for 4 min, followed by a ramp rate of 6 ℃/min to 280 ℃ and held for 5 min. The sample was injected at 280 ℃ of inlet temperature using a split

injection mode with a split ratio of 50:1, and the total flow rate was 54.1 mL/min. High purity helium (99.99%) was used as the carrier gas. EI (Electron ionization) ion source was used in MS with an energy level of 70 ev, and the temperature was 270 ℃. The MS scan range was 35-500 m/z, and the scan time interval was 0.3 s, and the scan speed was 1666. The peaks were identified and analysed based on NIST mass spectrometry library and literature.

2.4 Kinetic method

The analysis of pyrolysis kinetics helps to better understand the thermal degradation process, reaction mechanism and predict reaction pathways. In this study, Coats-Redfern method was mainly used for biomass pyrolysis reaction kinetics[26], and its method is derived based on formula (1):

$$\frac{d\alpha}{dt} = kf(\alpha) = A\exp[-E/(\mathrm{R}T)]f(\alpha) \quad (1)$$

$$\alpha = \frac{W_0 - W_\mathrm{t}}{W_0 - W_f} \quad (2)$$

$$\beta = \frac{\mathrm{d}T}{dt} \quad (3)$$

Where α is the conversion rate, W_0 is the initial mass of the sample, W_t is the mass of the sample at time t, W_f is the remaining mass of the sample at the end of the reaction, t is the reaction time, T is the absolute temperature, T is the rate constant of Arrhenius chemical reaction, $f(\alpha) = (1-\alpha)^n$ is the reaction mechanism function, and k is expressed as: $k = Ae^{-\frac{E}{\mathrm{R}T}}$.

By integrating equation (1) and substituting (3) into it, we get the following result:

$$G(\alpha)=\int_0^{\alpha}\frac{\mathrm{d}\alpha}{f(\alpha)}=\frac{A}{\beta}\int_0^{T}\exp\left(-\frac{E}{\mathrm{R}T}\right)\mathrm{dt} \quad (4)$$

By using the Coats-Redfern method, it is transformed to:

$$\frac{d\alpha}{dT}=\frac{A}{\beta}\exp\left(-\frac{E}{\mathrm{R}T}\right)(1-\alpha)^{n} \quad (5)$$

Where A is the pre-exponential factor, E is the reaction activation energy, n is the reaction order, R is general gas constant (8.314J/(K·mol)), T is the pyrolysis reaction temperature, and β is the heating rate, K/min.

When n=1,

$$\ln\left[\frac{-\ln(1-\alpha)}{T^2}\right]=\ln\left[\frac{A\mathrm{R}}{\beta E}\left(1-\frac{2\mathrm{R}T}{E}\right)\right]-\frac{E}{\mathrm{R}T} \quad (6)$$

When $n\neq1$,

$$\ln\left[\frac{1-(1-\alpha)^{1-n}}{T^2(1-n)}\right]=\ln\left[\frac{A\mathrm{R}}{\beta E}\left(1-\frac{2\mathrm{R}T}{E}\right)\right]-\frac{E}{\mathrm{R}T} \quad (7)$$

In general, $2RT/E$ is much less than 1, so the first term in the right end of the Coats-Redfern equation is almost constant. For biomass pyrolysis reaction, fitted linear lines of $\ln[-\ln(1-\alpha)/T^2]$ versus $1/T$ (n=1) and $\ln\{[1-\ln(1-\alpha)^{1-n}]/[T^2(1-n)]\}$ versus $1/T$ ($n\neq1$) can be plotted, and the frequency factor (A) and activation energy (E) can be calculated from the slope and intercept.

2.5 Synergistic effect calculation

In order to further analyse the interaction of C.V and PP during co-pyrolysis, the synergistic effect was calculated as the difference between the experimental value and theoretical value of co-pyrolysis (e.g.:weight loss, reaction activation energy, and relative peak area of the product):

$$Y_{diff} = Y_{exp.mix} - Y_{cal.mix} \quad (8)$$

$$Y_{cal.mix} = X_{c.v} Y_{exp.c.v} + X_{pp} Y_{exp.pp} \quad (9)$$

Where $X_{c.v}$ and X_{pp} represent the mass percentages of C.V and PP in the mixture, respectively. $Y_{exp.c.v}$ and $Y_{exp.pp}$ are the experimental values of C.V and PP, respectively. $Y_{exp.mix}$ and $Y_{cal.mix}$ are the experimental and theoretical values of the mixed sample, respectively. The positive and negative values of Y_{diff} are expressed as different synergistic effects (promotion or inhibition).

3 Results and discussion

3.1 Pyrolysis of C.V and PP for weight loss characteristics

Fig. 1 shows the co-pyrolysis TG and DTG curves of mixed samples of C.V and PP in different proportions at a heating rate of 20 ℃/min. It can be seen from Fig. 1 and Table 2 that the individual weight loss curves of C.V and PP were similar to those in the literature [11, 19]. According to the TG and DTG curves of C.V, the pyrolysis process can be divided into three stages. In the first stage (150~230 ℃), the volatile was slowly evaporated, and the sample was initially decomposed into macromolecular organic matter and low volatile components when heated. The weight loss rate on the DTG curve was slow. In the second stage (230~535 ℃), the weight loss of C.V was 74.18%, which was mainly due to a series of decomposition reactions of organic matter, including decarboxylation, dehydroxylation and dehydration of protein, polysaccharide and lipid components. The first peak of DTG curve at this stage was 283 °C, which indicated the decomposition of protein and carbohydrates, and the second peak at 338 °C indicated the decomposition of lipids. In the third stage

(535~900 ℃), the pyrolysis reaction was relatively slow with only 5.26% mass loss. The weight loss was mainly due to the decomposition of residual carbon at high temperature and the slow formation of small molecular gas volatiles such as CO and CO_2.

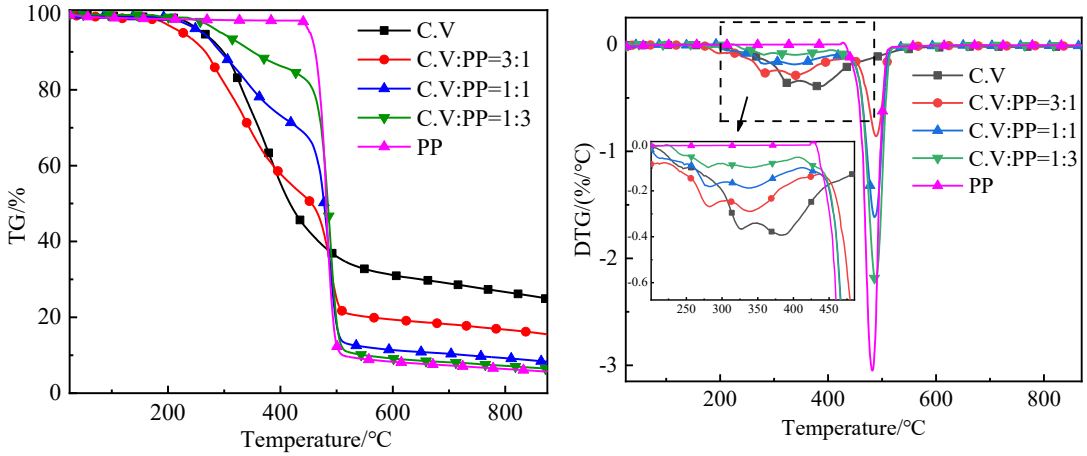

Fig. 1 TG and DTG curves of co-pyrolysis of C.V and PP at 20℃/ min heating rate.

Compared with C.V, the pyrolysis weight loss range of PP was relatively narrow, and its DTG curve only had a significant weight loss peak at 400-530 ℃. Its weight loss rate and maximum weight loss were significantly higher than those of microalgae. This is because PP has a high content of the volatiles than C.V, and they can be released in that pyrolysis temperature range. The DTG curve of co-pyrolysis showed that the first stage (250-410 ℃) was mainly the pyrolysis of C.V, and the peak temperature of pyrolysis weight loss in this stage was significantly decreased, which indicated that the addition of PP promoted the pyrolysis process of C.V and decreased its pyrolysis temperature [36]. However, the second stage (410-530 ℃) was mainly PP pyrolysis reaction. The DTG curve showed that the addition of C.V can slightly increase the peak

237 temperature of PP pyrolysis weight loss in this stage. The main reason for this
238 phenomenon was that the small molecules or free radicals released in the initial stage
239 of PP pyrolysis reacted with the residues produced by the pyrolysis of microalgae,
240 while the pyrolysis temperature of PP increases because of the lack of initiator [37].

241 Table 2 Pyrolysis characteristic parameters of individual samples and C.V/PP blends

Sample (C.V:PP)	t_b/℃	t_b/℃		t_t/℃	D_m/(%/℃)		Residue mass (%)
		P_1	P_2		P_1	P_2	
1:0	197	384	-	514	0.393	-	22.97
3:1	216	339	489	513	0.289	0.858	15.29
1:1	238	337	486	514	0.187	1.615	8.04
1:3	217	334	485	515	0.107	2.657	6.25
0:1	197	-	481	507	-	3.050	5.48

242 T_b: the start temperature,while the conversion ratio is 5*(1-x)%; p_n: n weight loss range;
243 t_m: the temperature while the weight loss ratio is largest; t_t: the final temperature
244 obtained by the cutting line method; D_m: the largest weight loss ratio

245 It can be seen from Fig. 2 that PP obviously promoted the pyrolysis of C.V within
246 220 ℃ to 400 ℃, and improved the weight loss rate in the main pyrolysis stage. There
247 was an obvious synergistic effect between the experimental value and the theoretical
248 value. This phenomenon was possibly due to the fact that PP disturbed the pyrolysis of
249 C.V to a certain extent, which made it more fully exposed to the pyrolysis space,
250 resulting in the pyrolysis weight loss rate of C.V increased and its pyrolysis
251 temperature shifted to lower values. In the temperature range of 400 to 482 ℃, with
252 the increase of PP mixing ratio, $\triangle W$ gradually changed from negative to positive value,
253 i.e. the positive synergy between them changed to negative synergy. The most possible
254 reason was that the small molecules of PP melt reacted with the pyrolytic residue of

C.V at the initial stage of PP pyrolysis, which led to a decrease of the initiator of PP pyrolysis and a shift of PP pyrolysis temperature to high values. However, when the temperature was higher than 482 ℃, the negative value of $\triangle W$ indicated a positive synergistic effect, which was mainly due to the partial overlap of pyrolysis temperature between C.V pyrolysis residue and PP. As a result, there were secondary reactions of PP and C.V pyrolysis coke, and the coke could promote the decomposition of PP into monomer or dimer, while PP could provide abundant hydrogen protons for the decomposition of C.V.

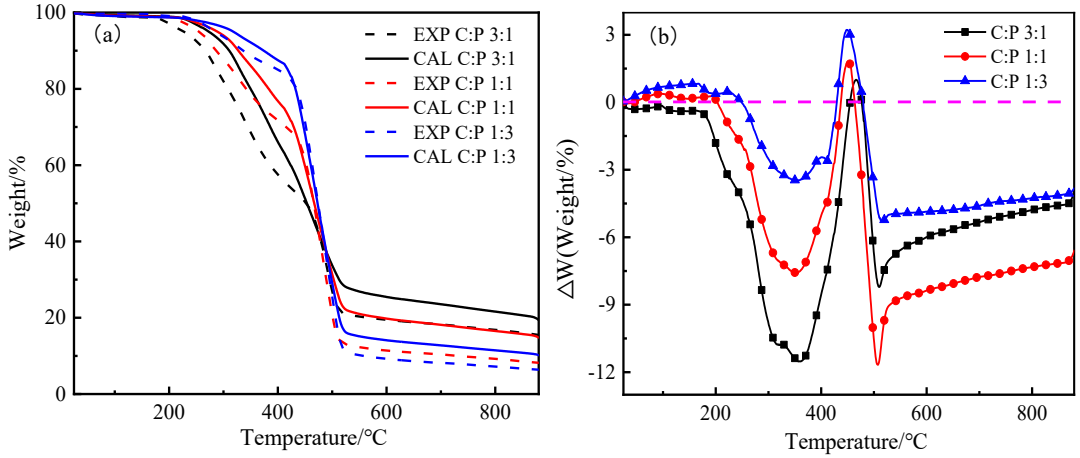

Fig. 2 (a) experimental and theoretical TG curve of the co-pyrolysis of C.V and PP and (b) weight difference value $\triangle W$.

3.2 Kinetic analysis of co-pyrolysis reaction between C.V and PP

The kinetic reaction parameters of C.V and PP alone and co-pyrolysis are shown in Table 3. When C.V and PP were co-pyrolysed, the temperature range was divided into three sections. The first two sections were mainly for the pyrolysis of C.V, while the third section was the main pyrolysis temperature range of PP. According to the calculation of Coats-Redfern method in Table 3, the pyrolysis reaction order of C.V and PP was 1. It can be seen that the pyrolysis of C.V alone was easier with an

activation energy of 40.09 kJ/mol, while the pyrolysis of PP alone was more difficult with a higher activation energy of 351.13 kJ/mol. As illustrated in Fig. 3, with the mixing ratio of PP increased from 0 to 1, the total activation energy of the reaction showed an increasing trend. Compared with the total activation energy and linear calculation activation energy, it was found that the energy required for co-pyrolysis of C.V and PP was significantly lower than that required for the individual pyrolysis. During the co-pyrolysis process, the difference between E_{ave} and E_{cal} increased from 64.56 kJ/mol to 81.80 kJ/mol with the mixing ratio of PP increased from 0.25 to 0.75. This phenomenon may be caused by the overlap of the distribution peaks on the activation energy plane produces an interaction during the C.V and PP of co- pyrolysis process.

Table 3 Pyrolysis kinetic parameters of individual samples and C.V/PP blends

Sample	Temperature/ （℃）	Weight loss （%）	E_{exp}/ (kJ·mol^{-1})	A/ （min^{-1}）	R^2	E_{ave}/ (kJ·mol^{-1})	E_{cal}/ (kJ·mol^{-1})
CV:PP 1:0	197-348	58.70	50.32	6.87× 10^3	0.9954	40.09	40.09
	348-420	18.95	39.22	4.52× 10^4	0.9980		
	420-514	22.35	13.98	1.28× 10^5	0.9801		
CV:PP 3:1	216-350	36.67	33.68	9.96× 10^4	0.9951	52.89	117.45
	350-461	26.50	8.43	2.99× 10^6	0.9813		
	461-513	36.83	104.00	9.20× 10^3	0.9812		
CV:PP 1:1	238-370	23.90	35.95	1.29× 10^5	0.9814	114.99	194.80
	370-458	14.12	7.95	6.12× 10^6	0.9813		
	458-514	61.98	169.86	4.10× 10^8	0.9817		
CV:PP 1:3	217-347	9.95	44.04	6.2× 10^4	0.9811	190.36	272.16
	347-456	11.27	9.77	1.18× 10^6	0.9746		
	456-515	78.78	234.68	1.20× 10^{13}	0.9864		
CV:PP 0:1	197-304	0.31	4.62	5.56× 10^8	0.9969	349.51	349.51
	304-432	0.16	8.47	2.26× 10^9	0.9936		
	432-507	99.53	351.13	1.89× 10^{21}	0.9886		

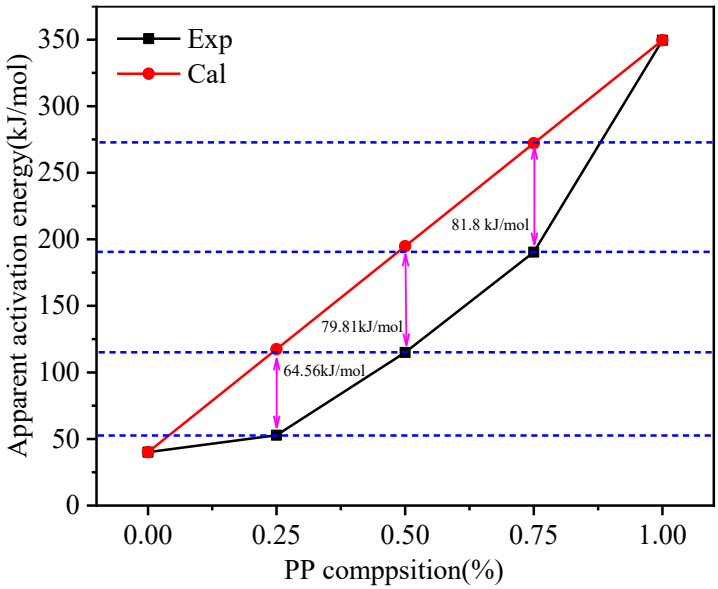

Fig. 3 Activation energy of PP and C.V for various samples.

3.2 Properties of liquid products (product distribution table and content variation diagram)

3.3.1 Effect of pyrolysis temperature on pyrolysis products of C.V

As can be seen from Table 4, the pyrolysis products of C.V were mainly composed of oxygenated compounds (acids, alcohols, ketones, esters, phenols, etc.), hydrocarbon (aromatics and aliphatic hydrocarbons), and nitrogenous compounds. Among them, oxygenated compounds showed the highest amount, which mainly included furfural, furan and ketone(produced by the decomposition of carbohydrate polysaccharides), phenolic compounds (formed by the decomposition of tyrosine in protein), and fatty acids, long-chain alcohols and esters (produced by ester bond fragmentation, decarboxylation and decarbonylation of triglycerides) [38]. Hydrocarbons (such as alkanes, olefins, toluene, etc.) were the second abundant, including aliphatic hydrocarbons mainly generated by the decomposition of lipids and the deoxygenation of sugars and aromatic hydrocarbons from the decomposition and aromatisation of

299 phenylalanine in microalgae proteins. Nitrogen-containing compounds were mainly
300 composed of indole derivatives formed by the thermal decomposition of tryptophan,
301 pyrrole, pyridine and amide derivatives formed by the pyrolysis of serine and
302 asparagine [39].

303 Table 4 List of bio-oil compounds presented in bio-oil.

Groups	Compounds	Formula	Compounds	Formula
Aromatic hydrocarbons	Toluene	C_7H_8	Benzene, propenyl	C_9H_{10}
	Styrene	C_8H_8	Benzene, propyl	C_9H_{12}
	p-Xylene	C_8H_{10}	Benzene, pentyl	$C_{11}H_{16}$
	Ethylbenzene	C_8H_{10}	TDN	$C_{13}H_{16}$
Aliphatic hydrocarbons	1,5-Heptadiene	C_7H_{12}	1,15-Hexadecadiene	$C_{16}H_{30}$
	D-Limonene	$C_{10}H_{16}$	Hexadecane	$C_{16}H_{32}$
	1,9-Decadiene	$C_{10}H_{18}$	1-Heptadecene	$C_{17}H_{34}$
	1-Decene	$C_{10}H_{20}$	Heptadecan	$C_{17}H_{36}$
	3-Undecene, 3-methyl-	$C_{12}H_{24}$	1-Nonadecene	$C_{19}H_{38}$
	Dodecane	$C_{12}H_{26}$	1,19-Icosadiene	$C_{20}H_{38}$
	1-Tridecene	$C_{13}H_{26}$	3-Icosyne	$C_{20}H_{38}$
	7-Tetradecyne	$C_{14}H_{26}$	(2E)-3,7,11,15-Tetramethyl-2-hexadecene	$C_{20}H_{40}$
	1-Tetradecene	$C_{14}H_{28}$	Heneicosane	$C_{20}H_{42}$
	Tetradecane	$C_{14}H_{30}$	Heneicosane	$C_{21}H_{44}$
	1,1,3-Trimethyl-2-(3-methylpentyl)cyclohexane	$C_{15}H_{30}$	1,21-Docosadiene	$C_{22}H_{42}$
	Pentadecane	$C_{15}H_{32}$	Tetracosane	$C_{24}H_{50}$
Nitrogenous compounds	Pyrrole	C_4H_5N	4-Ethyl-2-methyl-1H-pyrrole	$C_7H_{11}N$
	Aziridine, 1-ethenyl-	C_4H_7N	4-Methylcyclohexylamine	$C_7H_{15}N$
	Pyridine	C_5H_5N	Benzyl nitrile	C_8H_7N
	4(1H)-Pyrimidinone, 6-methyl-	$C_5H_6N_2O$	Indole	C_8H_7N
	1H-Pyrrole, 3-methyl	C_5H_7N	Pyrrole, 3-ethyl-2,4-dimethyl- 2,4-	$C_8H_{13}N$
	Isovaleronitrile	C_5H_9N	Benzenepropanenitrile	C_9H_9N
	Pyridine, 3-methyl	C_6H_7N	Indole, 3-methyl	C_9H_9N
	Pyrrole, 2,4-dimethyl	C_6H_9N	2-Ethyl-3,4,5-trimethyl-1H-pyrrole	$C_9H_{15}N$
	Isoamyl cyanide	$C_6H_{11}N$	Hexadecanamide	$C_{16}H_{33}NO$
	Pyridine, 2-ethyl	C_7H_9N	Heptadecanenitrile	$C_{17}H_{33}N$
Oxygenated compounds	Furfural	$C_5H_4O_2$	Cedrol	$C_{15}H_{26}O$
	Furfuryl alcohol	$C_5H_6O_2$	Hexa-hydro-farnesol	$C_{15}H_{32}O$

	Phenol	C_6H_6O	(Z)-11-Hexadecen-1-ol		$C_{16}H_{32}O$
	2-Furancarboxaldehyde, 5-methyl-	$C_6H_6O_2$	9-Octadecen-1-ol		$C_{18}H_{36}O$
	Furan, 2,5-dimethyl	C_6H_8O	1-Nonadecanol		$C_{19}H_{40}O$
	p-Cresol	C_7H_8O	Oleyl alcohol , acetate		$C_{20}H_{38}O_2$
	Coumaran	C_8H_8O	Phytol		$C_{20}H_{40}O$
	Phenol, 3-ethyl	$C_8H_{10}O$	Dihydrophytol		$C_{20}H_{42}O$
	2-Cyclooctenone	$C_8H_{12}O$	Stearic acid, allyl ester		$C_{21}H_{40}O_2$
	Cyclohexanepropano	$C_{10}H_{14}O$	Phytol, R,R,R,(E)3,7,11,15	acetate	$C_{22}H_{42}O_2$
	Hexanoic acid, isobutyl ester	$C_{10}H_{20}O_2$	1-Heptacosanol		$C_{27}H_{56}O$
	7-Tridecanone	$C_{13}H_{26}O$	Octacosanol		$C_{28}H_{58}O$
Carboxylic Acids	Tetradecanoic acid	$C_{14}H_{28}O_2$	n-Hexadecanoic acid		$C_{16}H_{32}O_2$
	Oleic Acid	$C_{18}H_{34}O_2$			

According to the Py-GC/MS data of C.V, the distribution of peak area percentage of main compounds at different final pyrolysis temperatures was listed in Table 5, and the analysis was carried out in five categories: aromatic hydrocarbons, aliphatic hydrocarbons, oxygenated compounds, nitrogen compounds and acids.

Table 5 Comparison of bio-oil compositions from C.V pyrolysis at different temperatures

	300 ℃	400 ℃	500 ℃	600 ℃	700 ℃
Aromatic hydrocarbons（%）	2.37	16.59	14.53	19.66	18.82
Aliphatic hydrocarbons（%）	17.98	7.83	24.53	12.17	12.13
Nitrogenous compounds（%）	11.42	22.03	20.46	22.33	27.14
Oxygenous compounds（%）	61.92	49.41	36.25	44.08	40.39
Carboxylic acids（%）	6.31	4.14	4.23	1.76	1.52

It can be seen from Fig. 4 that the peak area percentage of hydrocarbons (aromatic and aliphatic hydrocarbons) increased first and then decreased with the increase of the final pyrolysis temperature of C.V, and the maximum peak area percentage was 39.06% at 500 ℃. The reduction of hydrocarbons at high temperatures was attributed to the

secondary cracking of C.V and the formation of gaseous products. The fluctuation trend of nitrogen compounds in bio-oil was observed. It was found that the lowest peak area percentage ratio was 11.42% at 300 ℃ and the highest one was 27.14% at 700 ℃， which was mainly due to the release of volatile compounds from the solid phase, which led to the transfer of nitrogen elements to the liquid phase at a high temperature. Secondly, the coexistence of carbohydrates (acids) and proteins (amino acids) resulted in the Maillard reaction, which caused the thermochemical conversion of protein (amino acids) and carbohydrates (carbonyl) units into heterocyclic amines in C.V. Therefore, the content of nitrogen compounds in bio-oil fluctuates between different pyrolysis temperatures （ Amino acids→(pyridine, indole, pyrrole) and amides→nitriles).

In addition, with the increase of pyrolysis temperature, the acidic compounds and oxygen-containing compounds, including palmitic acid, myristic acid and oleic acid decreased significantly. The oxygen-containing compounds from C.V pyrolysis were mainly alcohols, phenols, ketones, aldehydes, esters and furans. Therefore, the reduced oxygen content in the obtained bio-oil was partly due to decarboxylation and decarbonylation of carboxyl and carbonyl compounds. Consequently, the release of H_2O, CO_2 and CO increased at high temperatures. As shown in Fig. 4, it was found that the oxygen-containing compounds in the bio-oil from C.V pyrolysis at 500 ℃ had the lowest relative peak area percentage of 36.25%, which had the maximum yield of hydrocarbon compounds [40].

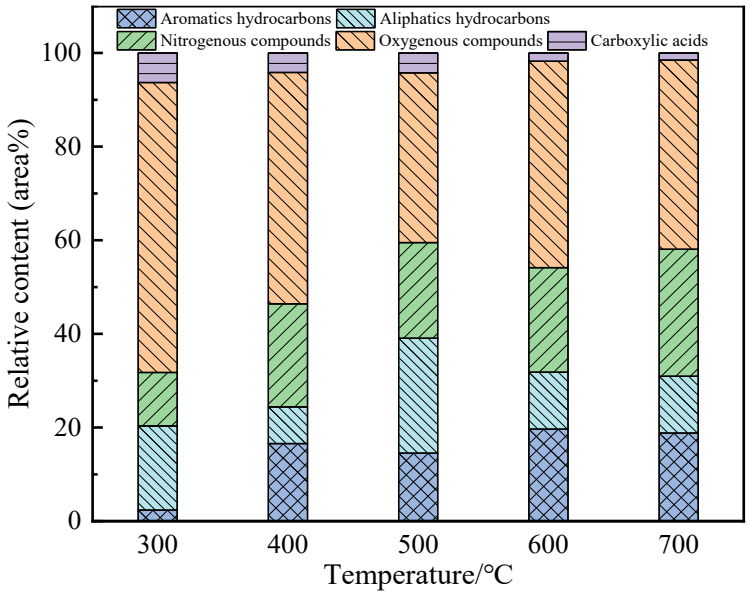

336

337 Fig. 4 Product selectivity of bio-oil compounds produced from pyrolysis of C.V at

338 different pyrolysis temperatures.

339 3.3.2 Effect of PP on pyrolysis products of C.V

340 As shown in Fig. 5, it was found that the distribution of pyrolysis products of C.V

341 and PP was significantly different. C.V had a high proportion of oxygen-containing

342 and nitrogen-containing compounds, while 93.22% of bio-oil from PP pyrolysis were

343 aliphatic hydrocarbons.

344 By comparing the distribution of pyrolysis products from C.V/PP mixtures and the

345 pure samples, it was found that the content of hydrocarbons increased significantly

346 even at low PP blending ratio, and the relative peak area percentage of hydrocarbons

347 increased with the increase of PP blending ratio. The main reason was that PP had high

348 C and H contents, low O content and no N element. Therefore, with the addition of PP,

349 the C/H ratio of mixed raw materials was improved, and thus the content of

350 hydrocarbons in liquid product was increased. In addition, the free radicals (-CH-, -

351 CH_2- and -CH_3-) released from PP pyrolysis could also promote the cracking and

decarboxylation of protein and carbohydrateto to form chain hydrocarbons, resulting in a significant increase in aliphatic hydrocarbon content [41]. At the same time, the peak area percentage of oxygen compounds, nitrogen compounds and acids decreased with the increase of the mixing ratio of PP. This was because that the introduction of PP inhibited the conversion of organic acids to alcohols, but promoted their decomposition to generate hydrocarbons. The interaction between PP and C.V inhibited the production of phenol, and the free radicals released by PP reacted with carbohydrates to generate hydrocarbons, resulting in the decrease of acids and oxygen-containing components. Nitrogen compounds (indole, nitrile, amine and other derivatives) was mainly produced by Maillard reaction of amino acids and reduced sugars [41]. The addition of PP would prevent Maillard reaction, promote the transfer of nitrogen into gas products instead of bio-oil, and finally lead to a reduction of nitrogen compounds in liquid products.

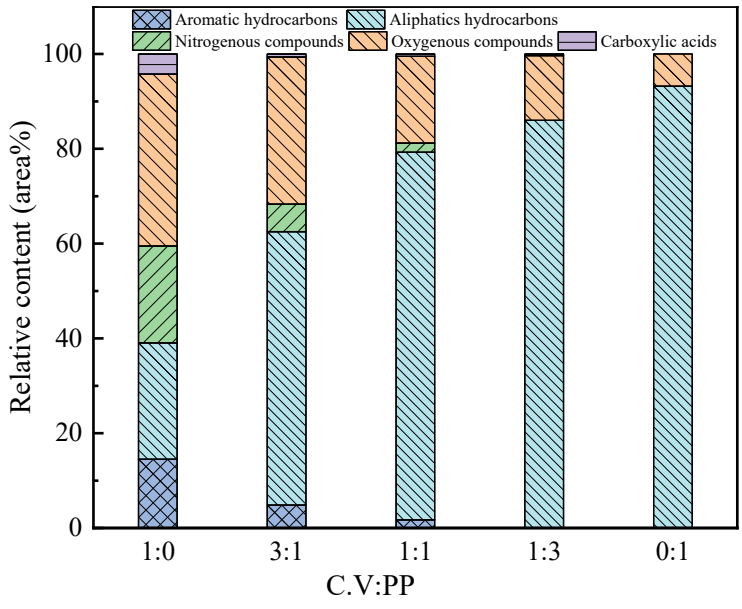

Fig. 5 Distribution of products in bio-oil prepared by C.V and PP at different mixing ratios.

368 3.3.3 Synergic effect and mechanism of liquid product distribution of PP and *Chlorella*
369 co-pyrolysis

370 From Fig. 6, it was found that the interaction between C.V and PP was beneficial
371 to promote the formation of hydrocarbons and improve the quality of pyrolysis
372 products by comparing the experimental and theoretical values of peak area of co-
373 pyrolysis products. Combing with the analysis of the pyrolysis characteristics of C.V
374 and PP, it can be seen that the free radicals released by PP promoted the decomposition
375 of protein and carbohydrates to form chain hydrocarbons. It was observed that when
376 the ratio of C.V/PP was 3:1 (i.e. 75% of C.V and 25% of PP), the inhibition of
377 oxygenated compounds (furans, ketones, aldehydes, esters and phenols) production
378 and the enhancement of hydrocarbon formation were the strongest. In addition, the
379 interaction between them significantly reduced the content of BTEXs and nitrogen-
380 containing compounds and increased the content of alcohols. This was because the
381 pyrolysis of PP produced a large amount of diolefins and proton (H^+) donors, which
382 promoted the cracking of aromatic products and inhibited the cyclisation and
383 aromatisation reaction hydrocarbons. Besides, it also prevented the Maillard reaction
384 between amino acids and reduced sugars, and inhibited the transfer of nitrogen into
385 bio-oil. The increased amount of alcohols were due to the interaction of hydrocarbon
386 radicals from PP and the intermediates (esters, furans and ketones and aldehydes) from
387 the pyrolysis of carbohydrates in C.V [42].

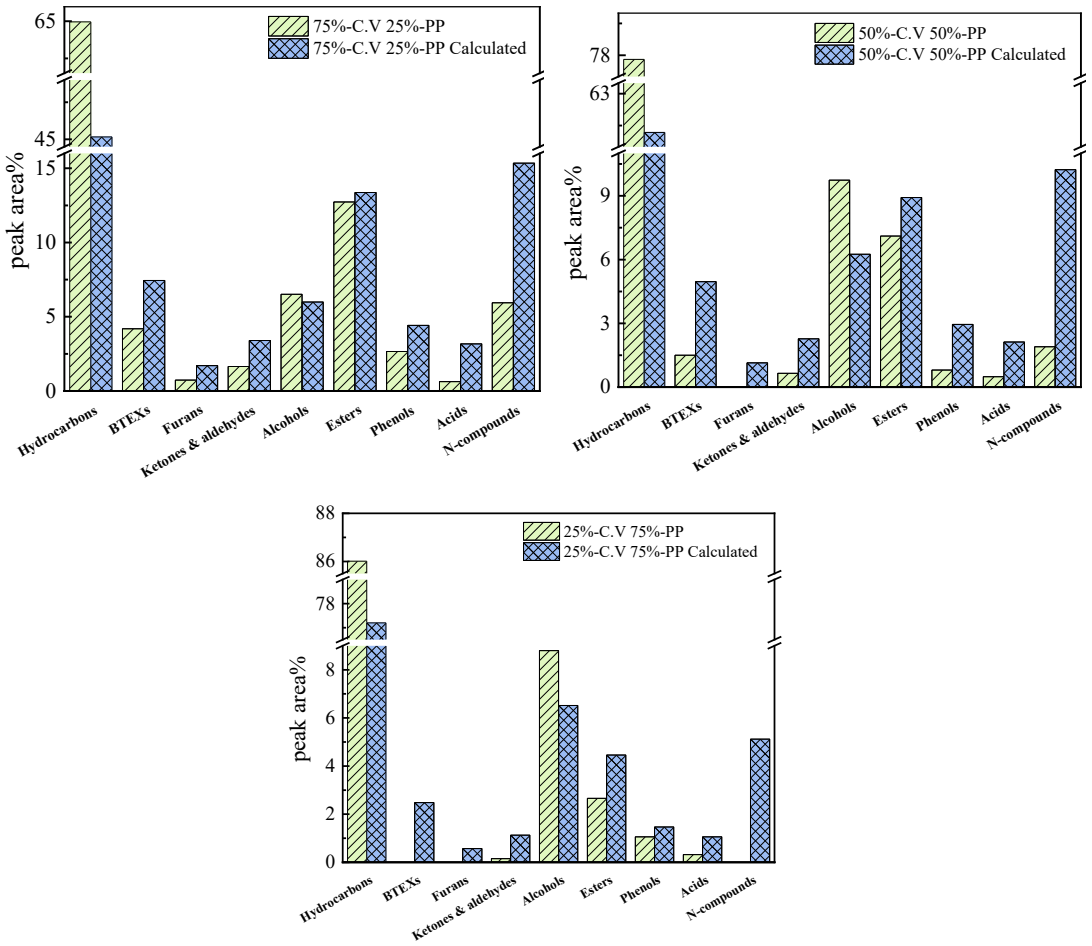

Fig. 6 Products from different ratio blends of C.V-PP by Py-GC/MS.

As shown in Fig. 7, the main components of C.V were protein, lipid and carbohydrate. The bio-oil detected by Py-GC/MS mainly consisted of amines, pyridines, pyrroles and nitriles compounds obtained from protein pyrolysis and alcohols, acids, esters and hydrocarbon compounds formed during lipid pyrolysis, and furans, aldehydes, ketones and hydrocarbons produced by carbohydrate pyrolysis.

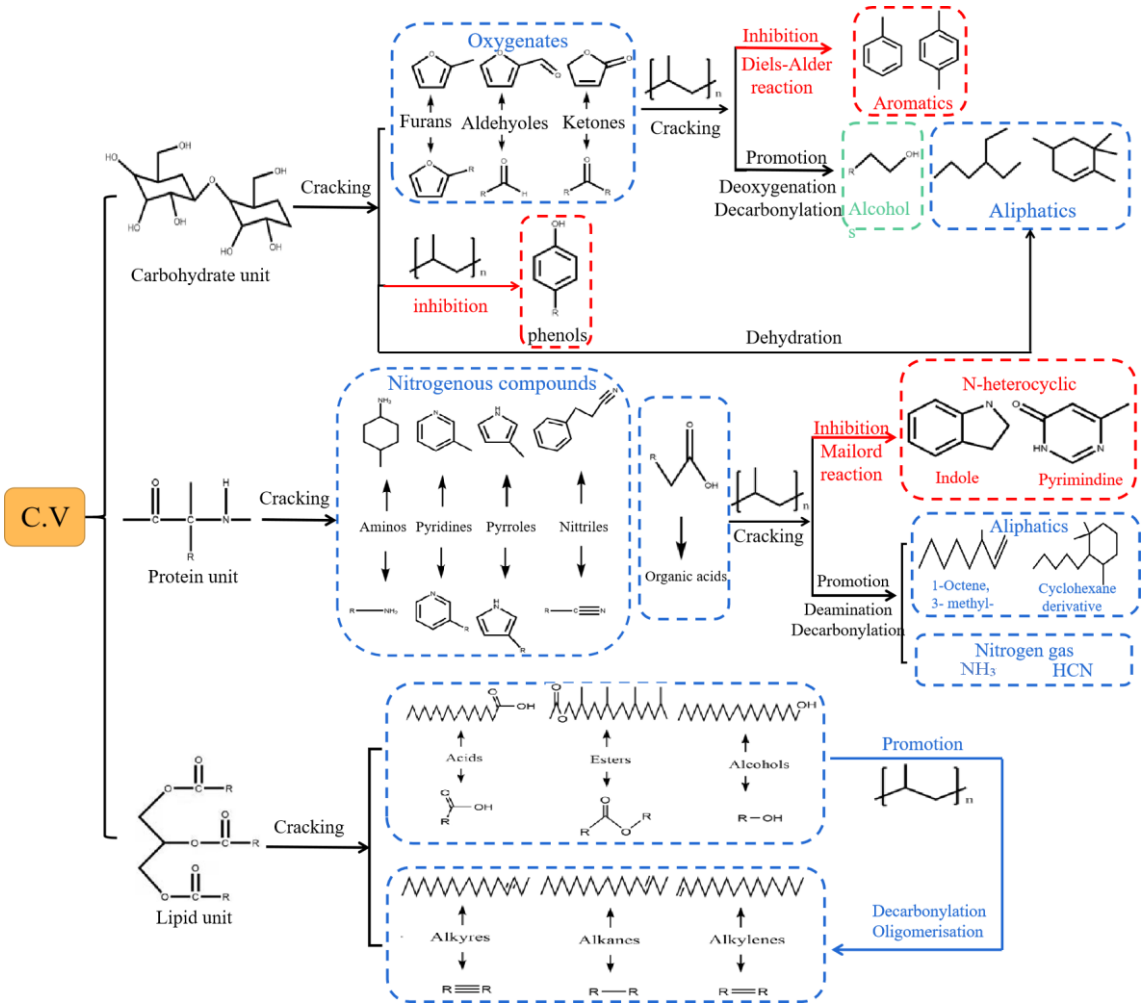

393 Fig. 7 Mechanism of interaction between C.V-PP co-pyrolysis.

394 After adding PP into C.V, the reaction mechanism could be summarised as below:

395 1) PP prevented the Diels-Alder reaction between olefins and inhibited the
396 production of phenol and aromatics, while the free radicals released by PP reacted with
397 furans, aldehydes and ketones to produce alcohols and hydrocarbons.

398 2) The hydrogen pool formed by PP pyrolysis could promote the interaction
399 between long-chain fatty acids and esters and H^+ free radicals to form a large amount
400 of long-chain hydrocarbons and long-chain alcohols.

401 3) The addition of PP inhibited the Maillard reaction between amino acids and
402 reduced sugars in protein to form indole and amide derivatives, leading to a reduction

403 of nitrogen-containing compounds and an enhancement of the formation of
404 hydrocarbons.

405 **4 Conclusions**

406 In this study, the co-pyrolysis behavior, reaction kinetics and product distribution
407 of C.V and PP were studied. The conclusions can be drawn as follows:

408 1) The co-pyrolysis of PP and C.V could be mainly divided into two stages. The
409 first stage was mainly C.V pyrolysis, and the peak temperature of pyrolysis decreased
410 significantly with the increase of PP blending ratio, and its weight loss temperature
411 range shifted significantly to a low temperature range. Compared with C.V, the second
412 stage was mainly the pyrolysis of PP, which showed an opposite treand. The synergistic
413 effect was enhanced, and the weight loss rate of pyrolysis at the final temperature was
414 further increased;

415 2) The results showed that the addition of PP could significantly reduce the
416 activation energy of the first and second stages of co-pyrolysis of PP and C.V, and
417 increased the activation energy of the third stage. The mixing ratio of PP played a
418 leading role in determining the activation energy of the reaction. The difference
419 between the experimental and theoretical activation energy of co-pyrolysis of C.V and
420 PP was 1:3 > 1:1 > 3:1, that was, when the mixing ratio of PP was 0.75, the activation
421 energy of the two had the best positive synergistic effect.

422 3) Py-GC/MS analysis showed that when the final pyrolysis temperature was
423 500 ℃, the peak area percentage of hydrocarbons in bio-oil produced by C.V reached
424 the maximum of 39.06%. When PP was co-pyrolysed with C.V, PP could significantly

promoted the deoxidation and denitrification of C.V pyrolysis products, and increased the yield of hydrocarbons. When PP blending ratio was 0.75, PP had the best synergistic effect on promoting the formation of aliphatic hydrocarbons and inhibiting the formation of aromatic hydrocarbons, nitrogen compounds, oxygen compounds and acids.

Acknowledgements

This work was supported by the Natural Science Foundation of China for Young Scholars (No.51706022，No.52006016), the Key Foundation of Hunan Educational Committee of China (No. 20A004). The authors also would like to acknowledge the funding from EU Horizon 2020 Research and Innovation Program under the Marie Skłodowska-Curie Action (Grant Agreement No. 823745).

References

[1] M.H.M. Ahmed, N. Batalha, H.M.D. Mahmudul, G. Perkins, M. Konarova, A review on advanced catalytic co-pyrolysis of biomass and hydrogen-rich feedstock: Insights into synergistic effect, catalyst development and reaction mechanism, Bioresour Technol 310 (2020) 123457.

[2] P. Ghorbannezhad, S. Park, J.A. Onwudili, Co-pyrolysis of biomass and plastic waste over zeolite- and sodium-based catalysts for enhanced yields of hydrocarbon products, Waste Manag 102 (2020) 909-918.

[3] F. Li, S.C. Srivatsa, S. Bhattacharya, A review on catalytic pyrolysis of microalgae to high-quality bio-oil with low oxygeneous and nitrogenous compounds, Renewable and Sustainable Energy Reviews 108 (2019) 481-497.

[4] H. Chowdhury, B. Loganathan, Third-generation biofuels from microalgae: a review, Current Opinion in Green and Sustainable Chemistry 20 (2019) 39-44.

[5] C. Yang, R. Li, B. Zhang, Q. Qiu, B. Wang, H. Yang, Y. Ding, C. Wang, Pyrolysis of microalgae: A critical review, Fuel Processing Technology 186 (2019) 53-72.

[6] S.Y. Teng，A.C.M. Loy, W.D. Leong, B.S. How, B.L.F Chin, V. Masa, Catalytic thermal degradation of Chlorella vulgaris: Evolving deep neural networks for optimization, Bioresour Technol 292 (2019)1241971.

[7] X.J. Lee, H.C. Ong, Y.Y. Gan, W.-H. Chen, T.M.I. Mahlia, State of art review on conventional and advanced pyrolysis of macroalgae and microalgae for biochar, bio-oil and bio-syngas production, Energy Conversion and Management 210 (2020).

[8] D. López-González, M. Puig-Gamero, F.G. Acién, F. García-Cuadra, J.L. Valverde, L. Sanchez-Silva, Energetic, economic and environmental assessment of the pyrolysis and combustion of microalgae and their oils, Renewable and Sustainable Energy Reviews 51 (2015) 1752-1770.

[9] P. Duan, X. Bai, Y. Xu, A. Zhang, F. Wang, L. Zhang, J. Miao, Non-catalytic hydropyrolysis of microalgae to produce liquid biofuels, Bioresour Technol 136 (2013) 626-34.

[10] N.H. Zainan, S.C. Srivatsa, F. Li, S. Bhattacharya, Quality of bio-oil from catalytic pyrolysis of microalgae Chlorella vulgaris, Fuel 223 (2018) 12-19.

468 [11] M.J.B. Fong, A.C.M. Loy, B.L.F. Chin, M.K. Lam, S. Yusup, Z.A. Jawad,
469 Catalytic pyrolysis of Chlorella vulgaris: Kinetic and thermodynamic analysis,
470 Bioresour Technol 289 (2019) 121689.
471 [12] W. Chen, Y. Chen, H. Yang, M. Xia, K. Li, X. Chen, H. Chen, Co-pyrolysis of
472 lignocellulosic biomass and microalgae: Products characteristics and interaction effect,
473 Bioresour Technol 245(Pt A) (2017) 860-868.
474 [13] J.T. Bong, A.C.M. Loy, B.L.F. Chin, M.K. Lam, D.K.H. Tang, H.Y. Lim, Y.H.Chai,
475 S. Yusup, Artificial neural network approach for co-pyrolysis of Chlorella vulgaris and
476 peanut shell binary mixtures using microalgae ash catalyst, Energy 207 (2020)118289.
477 [14] L. Chen, Z. Yu, J. Liang, Y. Liao, X. Ma, Co-pyrolysis of chlorella vulgaris and
478 kitchen waste with different additives using TG-FTIR and Py-GC/MS, Energy
479 Conversion and Management 177 (2018) 582-591.
480 [15] P. Duan, B. Jin, Y. Xu, F. Wang, Co-pyrolysis of microalgae and waste rubber tire
481 in supercritical ethanol, Chemical Engineering Journal 269 (2015) 262-271.
482 [16] Q. Xie, M. Addy, S. Liu, B. Zhang, Y. Cheng, Y. Wan, Y. Li, Y. Liu, X. Lin, P.
483 Chen, R. Ruan, Fast microwave-assisted catalytic co-pyrolysis of microalgae and scum
484 for bio-oil production, Fuel 160 (2015) 577-582.
485 [17] S. Magni, F. Bonasoro, C. Della Torre, C.C. Parenti, D. Maggioni, A. Binelli,
486 Plastics and biodegradable plastics: ecotoxicity comparison between polyvinylchloride
487 and Mater-Bi(R) micro-debris in a freshwater biological model, Sci Total Environ 720
488 (2020) 137602.

489 [18] M.L. Van Rensburg, S.p.L. Nkomo, T. Dube, The ‘plastic waste era’; social
490 perceptions towards single-use plastic consumption and impacts on the marine
491 environment in Durban, South Africa, Applied Geography 114 (2020).
492 [19] M. Tariq, D. Jinze, Z. Yaning, G. Mengmeng, L. Bingxi, Pyrolysis of plastic
493 species: A review of resources and products, Journal of Analytical and Applied
494 Pyrolysis 159 (2021) 105295.
495 [20] R.K. Singh, B. Ruj, A.K. Sadhukhan, P. Gupta, A TG-FTIR investigation on the
496 co-pyrolysis of the waste HDPE, PP, PS and PET under high heating conditions,
497 Journal of the Energy Institute 93(3) (2020) 1020-1035.
498 [21] R. Chen, J. Zhang, L. Lun, Q. Li, Y. Zhang, Comparative study on synergistic
499 effects in co-pyrolysis of tobacco stalk with polymer wastes: Thermal behavior, gas
500 formation, and kinetics, Bioresour Technol 292 (2019) 121970.
501 [22] M. Brebu, S. Ucar, C. Vasile, J. Yanik, Co-pyrolysis of pine cone with synthetic
502 polymers, Fuel 89(8) (2010) 1911-1918.
503 [23] K.G. Burra, A.K. Gupta, Kinetics of synergistic effects in co-pyrolysis of biomass
504 with plastic wastes, Applied Energy 220 (2018) 408-418.
505 [24] M. Alam, A. Bhavanam, A. Jana, J.k.S. Viroja, N.R. Peela, Co-pyrolysis of
506 bamboo sawdust and plastic: Synergistic effects and kinetics, Renewable Energy 149
507 (2020) 1133-1145.
508 [25] J. Gu H. Fan, Y. Wang, Y. Zhang, H. Yuan, Y. Chen, Co-pyrolysis of xylan and
509 high-density polyethylene: Product distribution and synergistic effects, Fuel 267
510 (2020).

511 [26] J.X. Liew, A.C.M. Loy, B.L.F. Chin, A. Alnouss, M. Shahbaz, T.Al-ansari, R.
512 Govindan, Y.H. Chai, Synergistic effects of catalytic co-pyrolysis of corn cob and
513 HDPE waste mixtures using weight average global process model, Renewable Energy
514 170 (2021)948-963.
515 [27] X. Kai, T. Yang, S. Shen, R. Li, TG-FTIR-MS study of synergistic effects during
516 co-pyrolysis of corn stalk and high-density polyethylene (HDPE), Energy Conversion
517 and Management 181 (2019) 202-213.
518 [28] H. Yuan, H. Fan, R. Shan, M. He, J. Gu, Y. Chen, Study of synergistic effects
519 during co-pyrolysis of cellulose and high-density polyethylene at various ratios,
520 Energy Conversion and Management 157 (2018) 517-526.
521 [29] M. Majid, B.L.F. Chin, Z.A. Jawad, Y.H. Chai, M.K. Lam, S. Yusup, K.W. Cheah,
522 Particle swarm optimization and global sensitivity analysis for catalytic co-pyrolysis
523 of Chlorella vulgaris and plastic waste mixtures, Bioresour Technol 329 (2021)124874.
524 [30] M. Dai, H. Xu, Z. Yu, S. Fang, L. Chen, W. Gu, X. Ma, Microwave-assisted fast
525 co-pyrolysis behaviors and products between microalgae and polyvinyl chloride,
526 Applied Thermal Engineering 136 (2018) 9-15.
527 [31] B. Cao, Y. Sun, J. Guo, S. Wang, J. Yuan, S. Esakkimuthu, B. Bernard Uzoejinwa,
528 C. Yuan, A.E.-F. Abomohra, L. Qian, L. Liu, B. Li, Z. He, Q. Wang, Synergistic effects
529 of co-pyrolysis of macroalgae and polyvinyl chloride on bio-oil/bio-char properties
530 and transferring regularity of chlorine, Fuel 246 (2019) 319-329.
531 [32] Z. Tang, W. Chen, Y. Chen, H. Yang, H. Chen, Co-pyrolysis of microalgae and
532 plastic: Characteristics and interaction effects, Bioresour Technol 274 (2019) 145-152.

533 [33] Z. Tang, W. Chen, J. Hu, S. Li, Y. Chen, H. Yang, H. Chen, Co-pyrolysis of
534 microalgae with low-density polyethylene (LDPE) for deoxygenation and
535 denitrification, Bioresour Technol 311 (2020) 123502.
536 [34] B.B. Uzoejinwa, X. He, S. Wang, A. El-Fatah Abomohra, Y. Hu, Q. Wang, Co-
537 pyrolysis of biomass and waste plastics as a thermochemical conversion technology
538 for high-grade biofuel production: Recent progress and future directions elsewhere
539 worldwide, Energy Conversion and Management 163 (2018) 468-492.
540 [35] X. Wu, Y. Wu, K. Wu, Y. Chen, H. Hu, M. Yang, Study on pyrolytic kinetics and
541 behavior: The co-pyrolysis of microalgae and polypropylene, Bioresour Technol 192
542 (2015) 522-8.
543 [36] X. Li, H. Zhang, J. Li, L. Su, J. Zuo, S. Komarneni, Y. Wang, Improving the
544 aromatic production in catalytic fast pyrolysis of cellulose by co-feeding low-density
545 polyethylene, Applied Catalysis A: General 455 (2013) 114-121.
546 [37] Z. Du, B. Hu, X. Ma, Y. Cheng, Y. Liu, X. Lin, Y. Wan, H. Lei, P. Chen, R. Ruan,
547 Catalytic pyrolysis of microalgae and their three major components: carbohydrates,
548 proteins, and lipids, Bioresour Technol 130 (2013) 777-82.
549 [38] F. Sotoudehniakarani, A. Alayat, A.G. McDonald, Characterization and
550 comparison of pyrolysis products from fast pyrolysis of commercial Chlorella vulgaris
551 and cultivated microalgae, Journal of Analytical and Applied Pyrolysis 139 (2019)
552 258-273.
553 [39] B. Nejati, P. Adami, A. Bozorg, A. Tavasoli, A.H. Mirzahosseini, Catalytic
554 pyrolysis and bio-products upgrading derived from Chlorella vulgaris over its biochar

555 and activated biochar-supported Fe catalysts, Journal of Analytical and Applied
556 Pyrolysis 152 (2020).
557 [40] X. Lv, H. Liu, Y. Huang, J. Yao, H. Yuan, X. Yin, C. Wu, Synergistic effects on
558 co-pyrolysis of low-temperature hydrothermally pretreated high-protein microalgae
559 and polypropylene, Energy Conversion and Management 229 (2021).
560 [41] X. Wang, X. Tang, X. Yang, Pyrolysis mechanism of microalgae Nannochloropsis
561 sp. based on model compounds and their interaction, Energy Conversion and
562 Management 140 (2017) 203-210.
563 [42]D.V.Suriapparao, B.Boruah, D. Raja, R. Vinu, Microwave assisted co-pyrolysis of
564 biomasses with polypropylene and polystyrene for high quality bio-oil production,
565 Fuel Processing Technology 175 (2018) 64-75.
566